JOURNAL OF THE MECHANICAL BEHAVIOR OF BIOMEDICAL MATERIALS 40 (2014) 413–425

Available online at www.sciencedirect.com

ScienceDirect

www.elsevier.com/locate/jmbbm

Research Paper

In vitro assessment of three dimensional dense chitosan-based structures to be used as bioabsorbable implants

Nuno Guitian Oliveira[a,b,c,*], *Tatiana Sirgado*[d], *Luís Reis*[a], *Luís F.V. Pinto*[b,e], *Cláudia Lobato da Silva*[c,d], *Frederico Castelo Ferreira*[c,d], *Alexandra Rodrigues*[a,f]

[a]*ICEMS, Instituto Superior Técnico, Universidade de Lisboa, Av. Rovisco Pais, 1049-001 Lisboa, Portugal*
[b]*Altakitin S.A., Rua José Gomes Ferreira, Arm. D, 2660-360 São Julião do Tojal, Lisboa, Portugal*
[c]*MIT Portugal Program, IST-Tagus Park, Av. Professor Cavaco Silva, 2744-016 Porto Salvo, Portugal*
[d]*Department of Bioengineering and IBB-Institute for Bioengineering and Bioscience, Instituto Superior Técnico, Universidade de Lisboa, Av. Rovisco Pais, 1049-001 Lisboa, Portugal*
[e]*CENIMAT/I3N, Departamento de Ciência dos Materiais, Faculdade de Ciências e Tecnologia FCT, Universidade Nova de Lisboa, Campus da Caparica, 2829-516 Caparica, Portugal*
[f]*GI-MOSM, Instituto Superior de Engenharia de Lisboa, ISEL, Rua Conselheiro Emídio Navarro, 1959-007 Lisboa, Portugal*

ARTICLE INFO

Article history:
Received 9 July 2014
Received in revised form
30 August 2014
Accepted 8 September 2014
Available online 28 September 2014

Keywords:
Chitosan
Glycerol
Bioabsorbable implants
Enzymatic degradation
Cytotoxicity
Mechanical properties

ABSTRACT

Chitosan biocompatibility and biodegradability properties make this biopolymer promising for the development of advanced internal fixation devices for orthopedic applications. This work presents a detailed study on the production and characterization of three dimensional (3D) dense, non-porous, chitosan-based structures, with the ability to be processed in different shapes, and also with high strength and stiffness. Such features are crucial for the application of such 3D structures as bioabsorbable implantable devices. The influence of chitosan's molecular weight and the addition of one plasticizer (glycerol) on 3D dense chitosan-based products' biomechanical properties were explored. Several specimens were produced and *in vitro* studies were performed in order to assess the cytotoxicity of these specimens and their physical behavior throughout the enzymatic degradation experiments. The results point out that glycerol does not impact on cytotoxicity and has a high impact in improving mechanical properties, both elasticity and compressive strength. In addition, human mesenchymal stem/stromal cells (MSC) were used as an *ex-vivo* model to study cell adhesion and proliferation on these structures, showing promising results with fold increase values in total cell number similar to the ones obtained in standard cell culture flasks.

© 2014 Elsevier Ltd. All rights reserved.

*Corresponding author. Tel.: +351 913 433 306.
E-mail addresses: nguitian@mit.edu, nunoguitian@gmail.com (N. Guitian Oliveira).

http://dx.doi.org/10.1016/j.jmbbm.2014.09.014
1751-6161/© 2014 Elsevier Ltd. All rights reserved.

1. Introduction

Bioabsorbable implants have been used successfully in craniomaxillofacial, neurological, general surgical and orthopedic procedures. Their use continues to increase in orthopedic subspecialties such as sports medicine, foot and ankle surgery, shoulder surgery, and in the specialty of spine surgery (Wuisman and Smit, 2006; Mukherjee and Pietrzak, 2011). These implants were developed to eliminate the need of a second surgical intervention for removal of the devices. In addition, the possible risks of metallic implants, such as corrosion and stress-shielding, due to mechanical incompatibilities between host bone and metallic implants, as well as the limitations with radiographic follow-up, have been recognized and can be avoided (Böstman and Pihlajamäki, 2000; Abbah et al., 2009; Van Dijk et al., 2002). On the other hand, polymer-based implants allow optimal postoperative radiographic evaluation because of their radiolucency and the absence of artifacts associated with similar metallic devices exposed to advanced imaging equipments. Moreover, bioabsorbable polymeric implants may offer advantages with respect to bone healing because of their unique biomechanical properties. With a modulus of elasticity closer to that of bone and with its gradual degradable properties, bioabsorbable implants gradually decrease the stress shielding seen with rigid metallic implant systems (Robbins et al., 2004; Lippman et al., 2004). Thus, the primary advantage of these new bioabsorbable materials is that they confer initial and intermediate-term stability that is adequate for bony healing in various applications. This is followed by gradual implant degradation and resorption, ideally after biologic fixation has occurred. Thus, the load is gradually transferred to the healing bone as they degrade (Vaccaro et al., 2003). However, the mode and the extent of degradation for a polymer under a set of conditions have to be known to determine the suitability of the material for a given application (Hasirci et al., 2001). Therefore, the control of the rate and extent of degradability of a polymeric biomaterial is critical for its intended function. For instance, for an orthopedic fracture fixation application, where the implanted polymeric biomaterial is needed for a limited duration, the ideal rate of resorption or degradation should not exceed the rate of bone formation and the reduction of strength of the implant should match, as good as possible, the increase in tissue strength (Hasirci et al., 2001).

Although there are many benefits when using bioresorbable implants, there has been a concern about the potential inflammatory response due to bulk erosion, acidic byproducts, and poor clearance of some of these degradation products. Other reported complications with the use of these bioabsorbable materials include sterile sinus tract formation, osteolysis, synovitis and hypertrophic fibrous encapsulation (Vaccaro et al., 2003), which lead to one of the major drawbacks associated with absorbable implants—foreign-body reaction. Although the incidence of this reaction varies among the existing implants, it has been reported with most of the currently available materials (Ambrose and Clanton, 2004). Due to the improved biocompatibility and the non-toxic nature of their degradation products, natural polymers are likely to replace synthetic polymers for some applications. Among natural polymers, chitosan is currently receiving substantial attention due to its biomedical applications that have been widely studied owing to its excellent biocompatibility, biodegradability and osteoconductive properties (Park and Kim, 2010; Correia et al., 2011; Freier et al., 2005; Knaul et al., 1998; Khor and Lim, 2003).

Chitosan, a deacetylated derivative of chitin, can be one promising material as a temporary mechanical supporter for bone fractures and other orthopedic applications since it mimics the role of chitin in the exoskeleton of crustaceans, which is analogous to that of collagen in bone (Hu et al., 2004; Pu et al., 2012; Qu et al., 2011). Three-dimensional chitosan-based rods have been constructed via an *in situ* precipitated method (Wang et al., 2010; Oh and Hwang, 2013; Wang and Hu, 2010). In general, these materials induce a minimal foreign body reaction, with little or no fibrous encapsulation. Formation of normal granulation tissue associated with accelerated angiogenesis appears to be the typical course of the healing response. This immunomodulatory effect has been suggested to stimulate the incorporation of the implanted material by the host (Di Martino et al., 2005; Eglin and Alini, 2008). Degradation of chitosan is controlled by the residual amount of acetyl content and it can degrade rapidly *in vivo* according to its deacetylation degree. In addition, porosity of chitosan specimens can be controlled which can affect their strength and elasticity (Cheung et al., 2007; Chesnutt et al., 2009). Lysozyme is the primary enzyme responsible for *in vivo* degradation of chitosan through hydrolysis of acetylated residues (Di Martino et al., 2005). This enzyme breaks down the chitosan polymer chain, diminishing its molecular weight until it becomes small enough to be processed by cells. Lysozyme is abundant throughout the human body, being present in lymphocytes and also secreted by monocytes, macrophages, and granulocytes, which account for the largest source (Ralph et al., 1976). Monocytes and macrophages are the dominating contributors to the lysozyme content in serum (Martins et al., 2010). Lysozyme commonly exists in various human body fluids and tissues with concentrations from 4 to 13 mg/L in serum and from 450 to 1230 mg/L in tears (Ren et al., 2005). The degradation rate of chitosan is inversely related to the degree of crystallinity and therefore, highly deacetylated forms may last several months *in vivo*, being chitosan oligosaccharides of variable length the degradation products (Di Martino et al., 2005; Greenwald et al., 1972; Kim et al., 2008).

In order to improve elasticity and overcome problems associated with high deacetylated chitosan specimens' brittleness (Nunthanid et al., 2001), the addition of a plasticizer is possible. The main non-volatile plasticizers are glycerol, sorbitol, propylene glycol or polyethylene glycol (Domján et al., 2009; Zhang et al., 2002; Kolhe and Kannan, 2003). Among them, glycerol is the most used plasticizer due to its good plasticization efficiency, large availability and low exudation (Epure et al., 2011). Moreover, the strongly hydrogen-bonded chitosan/glycerol mixtures are as strong as or even stronger than when chitosan is used alone. Thus, glycerol is suggested to improve the processability of chitosan specimens and their mechanical properties (Quijada-Garrido et al., 2006).

Although chitosan has been proving to be one of the most promising biopolymers to be used in future generations of

implantable devices for orthopedic applications (Di Martino et al., 2005), there are few results regarding the production and characterization of dense, i.e. non-porous, chitosan-based structures able to be simultaneously easily machined in different shapes and able to support high loads. The high strength and stiffness associated to the dense structures under study are important features of biodegradable osteosynthesis devices, such as plates, screws or spinal cages. In a previous publication (Guitian Oliveira et al., 2013) the authors described a novel method for the production of 3D dense chitosan structures. The aim of this work is to present the results related to the cytotoxicity and *in vitro* enzymatic degradation studies that were performed in order to further assess the influence of chitosan molecular weight and the addition of glycerol in these 3D dense chitosan-based products. Preliminary experiments using human mesenchymal stem/stromal cells (MSC) were also conducted. These are adult multipotent cells, found in several connective tissues, in particular in the adult bone marrow niche and can differentiate into several tissues, including bone tissue (Caplan, 1991). Therefore, such cells were identified and used as model to assess cell proliferation in the 3D dense chitosan-based specimens.

2. Materials and methods

Medical grade chitosan from Altakitin S.A. (Portugal), with high molecular weight (800 kDa; 90% deacetylation degree; viscosity 1200 cps) and medium molecular weight (300 kDa; 90% deacetylation degree; viscosity 200 cps) were used without further purification. The glacial acetic acid and the sodium hydroxide solution (50% w/v) were purchased from Panreac Química S.L.U. Pharmaceutical grade glycerol (purity degree $\geq$99.5%) was purchased from AMSC. Lysobac, a recombinant human lysozyme produced in an animal-free production system, was purchased from Sigma-Aldrich.

2.1. Preparation and characterization of chitosan-based specimens

The fabrication process for the production of chitosan-based specimens involved the dissolution of free base chitosan powder (3%, w/v) alone, or with glycerol (7.5%, v/v), in an aqueous solution of acetic acid (2%, v/v). After total dissolution, the homogeneous solution was poured in 60 × 40 mm cylindrical molds and left at 5 °C overnight to remove air bubbles, prior to be frozen at −20 °C for 24 h. The frozen solutions were then removed from the molds and precipitated in a sodium hydroxide aqueous solution (10%, w/v) for 48 h. The specimens that resulted from the gelation process were abundantly washed with deionized water until pH~7 and dried in oven at 40 °C for 96 h. The three-dimensional dried and dense specimens were then machined into cylindrical structures with a diameter of approximately 14 mm and 6.5 mm height. Table 1 resumes the four different types of specimens that were prepared for this study.

2.1.1. Morphological analysis

The cross-sectional morphology of chitosan-based specimens was analyzed using a Hitachi Scanning Electron Microscope (SEM)/S 2400 (Hitachi Instruments, Inc.), at an accelerating voltage of 20 kV. A fine stream of carbon was previously deposited onto specimens due to their nonconductivity. Different cross sections areas were observed and analyzed in terms of porosity (size and distribution), topography and overall density.

Table 1 – Name and composition of chitosan-based specimens.

Specimens name	Molecular weight (Mw)	Glycerol (Gl)
H	High (800 kDa)	No
H+Gl	High (800 kDa)	Yes
M	Medium (300 kDa)	No
M+Gl	Medium (300 kDa)	Yes

2.1.2. NMR spectroscopy

The composition and the degree of deacetylation of the chitosan-based specimens were determined by ^{1}H NMR spectra, according to the method described by Hirai et al. (1991). Measurements were performed on a Bruker Avance-III 400 MHz NMR spectrometer, under a static magnetic field of 9.4 T at 70 °C. The software used to analyze the spectrum was the Bruker Topsin 3.1. The concentration of chitosan solution was 10 mg/mL in a DCl/D_2O solution (2%, w/v). The degree of deacetylation (DD) was evaluated by using the integral intensity of CH_3 residue (ICH_3) and the sum of integral intensities of H_2–H_6 ($I_{H2–H6}$) (1):

$$DD(\%) = \left\{1 - \left(\frac{1}{3} I_{CH3} / \frac{1}{6} I_{H2-H6}\right)\right\} \times 100 \quad (1)$$

2.1.3. Swelling ratio

The water sorption capacity of the produced specimens was determined by immersing them in phosphate buffered saline (PBS, Sigma-Aldrich) at pH 7.4 for 24 days at 37 °C. The swollen specimens were removed at predetermined time intervals (30 min, 1 h, 2 h, 4 h, 8 h, 24 h, 2 days, 3 days, 6 days, 12 days and 24 days) and immediately weighted with an analytical balance after the removal of excess of water by laying the specimens on a filter paper for 1 min. The swelling ratio (SR) was calculated using Eq. (2):

$$SR(\%) = (W_t - W_0)/W_0 \times 100 \quad (2)$$

where W_t and W_0 are the weights of the specimens at time t (swelling state) and at time 0 (dry state), respectively.

2.2. Enzymatic degradation of chitosan-based specimens

Prior to start this experiment, all the specimens were sterilized by immersing them in ethanol (70%, v/v), for 72 h, followed by UV exposure overnight. Ethanol was chosen as a sterilizer due to its negligible effect on the physical properties of materials, as reported in the literature (Albanna et al., 2013). Chitosan-based specimens were then placed in PBS (control) or in an enzymatic solution containing 500 mg/L of lysozyme and incubated (37 °C, 5% CO_2, fully humidified) for different time periods and the medium replaced every week.

At predetermined time intervals (15, 30, 45 and 60 days) specimens were taken from the solutions, washed with distilled water to remove salts and dried for 24 h at 40 °C.

2.2.1. Weight loss

The weight loss (WL) of the specimens was calculated according to Eq. (3):

$$WL(\%) = (W_i - W_f)/W_i \times 100 \quad (3)$$

where, W_i is the initial dry weight of the specimen and W_f is the weight of the dry specimen either after incubation in PBS, or in the enzymatic solution.

2.2.2. Mechanical properties

Mechanical compression tests of these specimens were performed, according to the ASTM D695 standard, using a universal testing machine from Instron (model 5566) equipped with a load cell of 10 kN and a crosshead speed of 1.5 mm/min. The results were processed with Bluehill® 2 Materials Testing Software. A nominal stress/strain curve was plotted in order to determine the specimens' modulus of elasticity and compressive strength. The nominal compressive stress was defined as the compressive load divided by the initial cross section area of the specimen, and the compressive strength was the maximum compressive stress supported by a test specimen. The compressive strain was defined as the change in length per unit of original length along the longitudinal axis and the compressive modulus of elasticity was calculated by the slope of the initial linear portion of the stress–strain curve.

2.3. In vitro cytotoxicity and cell proliferation on chitosan-based specimens

The specimens produced were tested for cytotoxicity according to the international standard ISO 10993-5:2009(E) for medical devices. Specimens were sterilized by immersing them in ethanol (70%, v/v), for 72 h, followed by UV exposure overnight. Triplicates of each type of specimen were placed in 6-well plates containing 2 mL of 10% (v/v) Iscove's Modified Dulbecco's Medium (IMDM) +10% (v/v) Fetal Bovine Serum (FBS) (both GibcoBRL, from Life Technologies) and incubated (37 °C, 5% CO_2, fully humidified). After 72 h of incubation, this medium was transferred to 24-well plates and used to culture mouse fibroblasts (L929 cell line, DSMZ Germany) for 48 h, plated at an initial density of 80×10^3 cells/cm^2. Fresh IMDM-10% FBS medium not exposed to any material was used as negative control and IMDM-10% FBS medium, which has been left 72 h in contact with a piece of latex glove used as positive control.

2.3.1. Cell metabolic activity

Cell metabolic activity was analyzed by using the 3-(4,5-dimethylthiazol-2-yl)-2,5-diphenyltetrazolium bromide (MTT) assay (Sigma) and the results were normalized to the negative control for cytotoxicity and compared to the positive control.

2.3.2. Cell morphology and confluence

In order to perform direct contact assays, L929 cells were plated on a 24-well plate, 20×10^3 cells per well for 72 h. Specimens were placed on the top of cell layers, with IMDM-10% FBS medium, and incubated (37 °C, 5% CO_2, fully humidified) for 48 h. The morphology and confluence of cells in contact with materials were analyzed by using an optical microscope.

2.3.3. Cell proliferation

Bone marrow MSC previously expanded for 5 passages were harvested and seeded on the chitosan specimens (previously incubated overnight with culture medium) at a cell density of 5000 cells/cm^2, as described elsewhere (Canadas et al., 2014). Assays were performed in triplicate. Medium used for MSC cultivation was Dulbecco's modified Eagle's medium (DMEM) (GibcoBRL) containing 10% FBS MSC-qualified (GibcoBRL), supplemented with streptomycin (0.025 mg/mL) and penicillin (0.025 U/mL) (GibcoBRL) and incubation always took place at 37 °C and 5% CO_2 in a humidified atmosphere. Cell numbers were estimated by AlamarBlue® test, according to manufacturer's instructions (O'Brien et al., 2000). Briefly, AlamarBlue® solution was diluted in medium, added to MSC cultures in chitosan, incubated for 2 h and fluorescence intensity measured (excitation wavelength, 560 nm; emission wavelength, 590 nm, read in a black 96-well plate 150 μL/well) for each condition. The value taken corresponds to cell's metabolic activity and it was converted into cell number following an established calibration curve. Negative control wells do not have cells.

2.4. Statistical analysis

Each experiment was carried out in triplicate unless otherwise specified. All results are presented as mean ± standard deviation (SD). Experimental data were analyzed using single-factor Analysis of Variance (ANOVA) technique to assess statistical significance of results. Independent-Sample *T*-test was adopted for statistical comparisons between two groups. In all statistical evaluations, statistical significance was set to p-value ≤ 0.05 (and labeled with **).

3. Results and discussion

The aim of this study is to assess the impact of different molecular weight chitosans and glycerol addition in the mechanical and biological properties of 3D dense chitosan-based products. The results related to the studies that were performed are detailed and discussed throughout the following subsections.

3.1. Characterization of chitosan-based specimens

During the preparation of specimens, the difference of viscosity between the high molecular weight chitosan (H) acid solution and the medium molecular weight (M) acid solution was notorious. Although it was possible to dissolve 3% (w/v) for both types of chitosan, H took twice the time to dissolve in 2% (v/v) acetic acid solution when compared to M due to its higher chain lengths, being the viscosity of H solution greater than the other. Similar results were obtained when preparing the H+Gl and M+Gl specimens. The testing specimens were prepared from cylindrical structures that were machined in a milling machine in order to give them smooth and parallel surfaces.

During this process, a highly differentiated behavior between plasticized and unplasticized specimens was observed. All specimens with glycerol were much easier to shape when comparing to the others. The unplasticized specimens presented a much more brittle behavior, due to the high degree of deacetylation of both chitosans used (Nunthanid et al., 2001), which occasionally led to cracking of some specimens.

In order to study the cross section morphology of the specimens, SEM analyses were conducted. As can be seen from Fig. 1, there is a significant difference between specimens with and without glycerol in their content. Thus, when comparing H with H+Gl, or M with M+Gl, it is notorious the difference in their microstructure, being the plasticized specimens more dense and without visible pores, while both H and M specimens presented a more irregular and rough surface with small and randomly distributed pores. Such behavior can be attributed to the strong H-bonds formed between glycerol and chitosan molecules and, on the other hand, to the cleavage of inter- and intramolecular H-bonds between chitosan chains, making them moving closer to each other (Bajdik et al., 2009).

Fig. 2a presents an example of an NMR spectrum. The DD was calculated according to Eq. (1) resulting in 90.8%, meaning that the degree of deacetylation of chitosan did not experience any alteration during the specimens production process, as previously reported (Guitian Oliveira et al., 2013). The resonances of the plasticizer can be detected beneath the signals of the chitosan (Fig. 2b).

There are numerous possibilities to form intra- and intermolecular H-bonds between chitosan's hydrogen-rich hydroxyl (–OH) and amine (NH_2) groups, and carbonyl groups and the plasticizer molecules (Domján et al., 2009). The acetamide group plays an important role in the formation of intermolecular bonds between adjacent chains. The proton environment of the carbonyl atoms does not change significantly when the plasticizer is added to chitosan specimens, meaning that the carbonyl polarization results predominantly from interaction with the chitosan hydrogen atoms (Domján et al., 2009). Glycerol is a very good H-bond donor and acceptor, and therefore it increases the number of H-bonds by donating protons to carbonyl groups and accepting chitosan OH and NH_2 protons (Domján et al., 2009). The amide NH proton is in close proximity to C3 carbon if the carbonyl group forms an H-bond with the OH group on C6 carbon. Glycerol molecules are probably bound to the acetamide group of chitosan by H-bonds, which prevent the acetamide groups from forming interchain H-bonds with other chitosan molecules, and leads to break down of the intermolecular connectivity between the polysaccharide chains (Domján et al., 2009).

As a general behavior, it is known that both plasticized and unplasticized chitosan samples have a great water sorption capacity through hydrogen bonds with some chitosan sites.

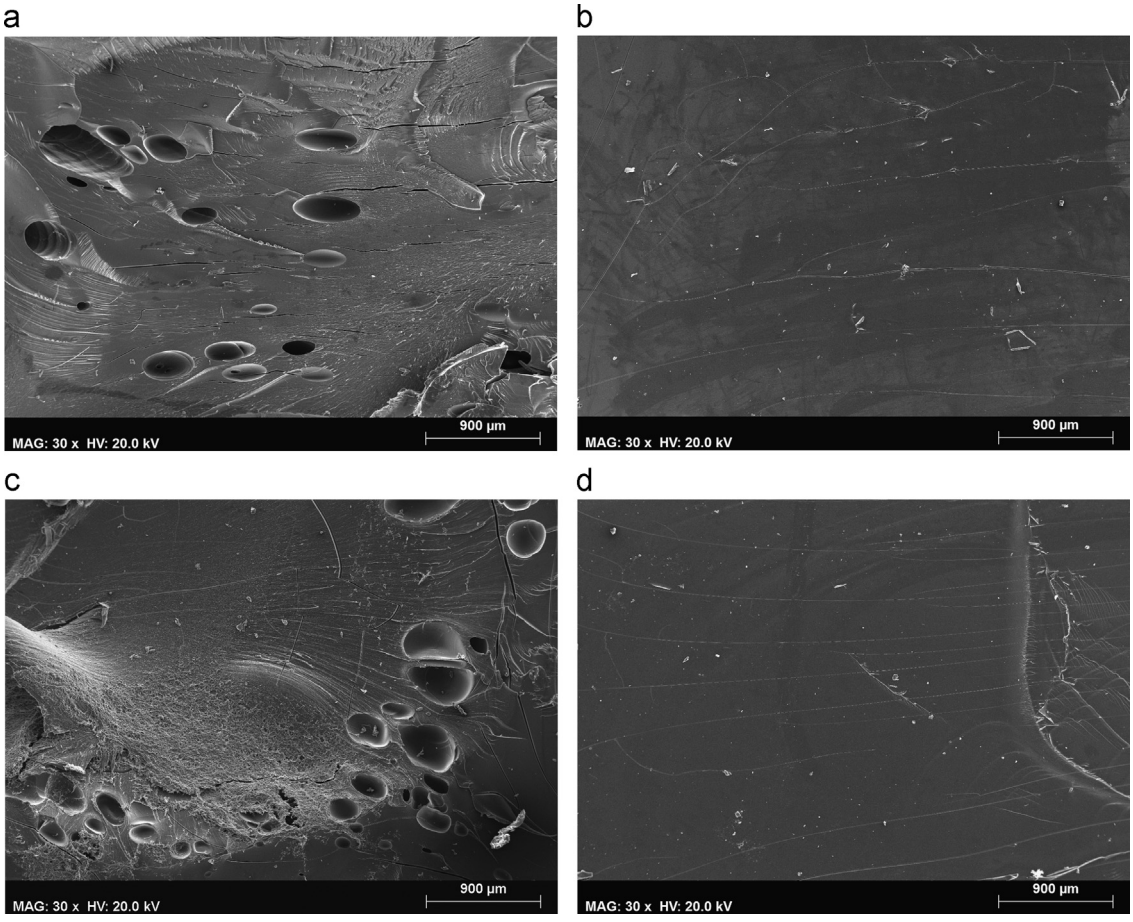

Fig. 1 – SEM images of 4 chitosan-based specimens: (a) H; (b) H+Gl; (c) M; (d) M+Gl.

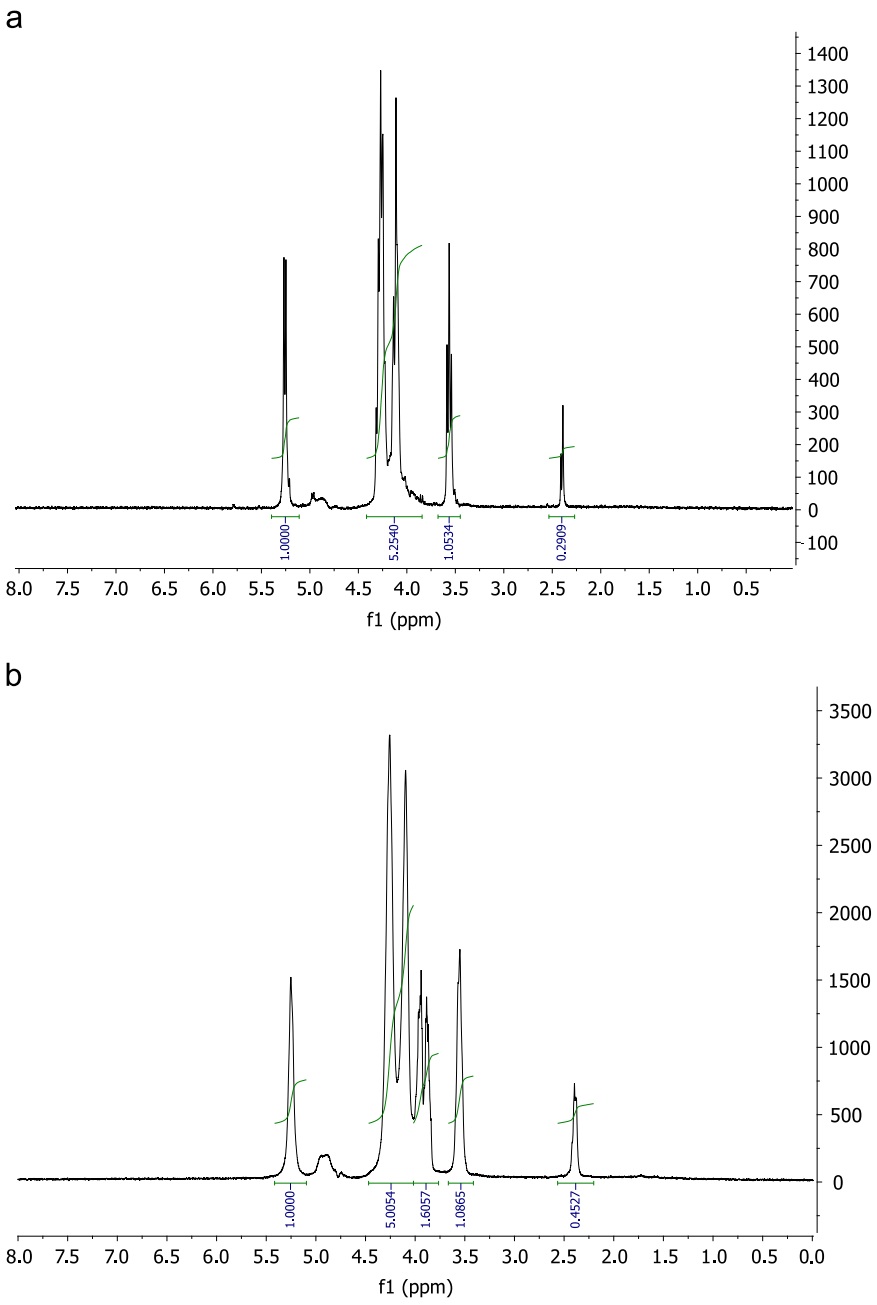

Fig. 2 – ^{1}H NMR spectrum of an H specimen (a) and an H+Gl specimen (b).

The swelling ratios for the four chitosan-based specimens are shown in Fig. 3, where it is visible that the majority of the water uptake took place in the first 2 days. When comparing the H-based and the M-based specimens, with and without glycerol, the highest water absorption values were obtained with unplasticized samples. As glycerol interacts through hydrogen bonds with chitosan and with water molecules, it was expected that it could lead to higher water contents (Epure et al., 2011); however, the porous microstructure of unplasticized specimens seems to favor the water uptake. On the other hand, the dense microstructure of plasticized specimens, as can be seen from SEM images, made them more swelling-resistance. Furthermore, the swelling ratio of H-based specimens was higher than the M-based ones. Thus, taking into account that both chitosans have the same deacetylation degree (DD), the results suggest that for the same DD, the lower the molecular weight of chitosan the lower the swelling rate of these chitosan-based specimens due to their easier chain rearrangements.

Increasing swelling-resistance of chitosan-based specimens can be considered a critical step to ensure its use as a functional load bearing material (Oh and Hwang, 2013). There are several approaches to decrease the swelling ratio of chitosan-based specimens. Adding hydroxyapatite, or cross-linking chitosan specimens (e.g. with glutaraldehyde or genipin) are some of the reported approaches to decrease their swelling ratio (Mi et al., 2001; De Souza Costa-Júnior et al., 2009; Silva et al., 2005). A heat treatment can also be an effective approach to prevent

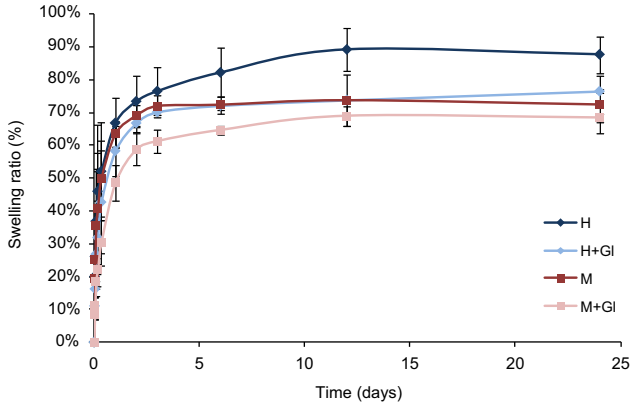

Fig. 3 – Swelling ratio (%) of 4 different chitosan-based specimens over 24 days.

swelling. This fact is attributed to the formation of a more rigid network after dehydration (Itoh et al., 2003). From the results, a similar behavior is obtained with plasticized specimens. Due to a more dense and rigid structure, these specimens presented a lower swelling ratio when compared to their unplasticized counterparts.

3.2. *Enzymatic degradation of chitosan-based specimens*

The *in vitro* degradation of chitosan-based specimens was conducted with lysozyme to mimic these specimens *in vivo* degradation behavior. However, a concentration of lysozyme much higher than the concentration in human serum was used. This approach follows previously reported studies (Correia et al., 2011; Ren et al., 2005; Reves et al., 2012; Nguyen et al., 2013) aiming to accelerate the degradation process, since a slow degradation rate was expected due to the high deacetylation degree (DD) of both chitosans. The DD highly influences the degradation behavior and mechanism by enzymes and is well known that the higher the DD of chitosan, the slower its degradation process becomes. Thus, highly deacetylated forms exhibit low degradation rates and may last several months *in vivo* (Freier et al., 2005; Ren et al., 2005; Kim et al., 2008; Reves et al., 2012; Nguyen et al., 2013; Lim et al., 2008; Nair and Laurencin, 2007).

Lysobac, the enzyme used in this study, is a recombinant human lysozyme produced in an animal-free production system. Animal-free production eliminates the safety risk and inconsistent lot-to-lot performance of the frequently used hen egg white lysozyme. Moreover, Lysobac has significantly higher bioactivity than hen egg white lysozyme since one gram of Lysobac roughly corresponds to 4 g of hen egg white lysozyme (Sigma-Aldrich).

The degradation of the different specimens was evaluated by estimation, over time, of their weight loss and mechanical properties. To distinguish between enzymatic degradation and non-enzymatic degradation, both the weight loss (Fig. 4) and the mechanical properties of specimens (Figs. 5 and 6) that had been placed in PBS supplemented with lysozyme were compared with those that had been placed in PBS used as a control solution (without enzyme).

Weight loss of chitosan-based specimens increased along with time of degradation, as expected (Hsieh et al., 2007). However, greater weight loss results were observed for non-plasticized H and M samples than for plasticized specimens. This higher degradation rate for non-plasticized specimens is most probably related to their microstructure, since the degradation rate of porous structures is expected to be faster than films or other nonporous structures forms, owing to the larger contact area with the degradation solution (Lim et al., 2008). Therefore, although the number and size of the randomly distributed pores in H and M specimens were small, such microstructure had a clear impact in their weight loss rate, which was greater in the first days than for H+GL and M+Gl: more than 8% weight loss, on average, after 15 days. Overall, the weight loss of all tested specimens significantly increased after 60 days. Taking into account the results, there is a notorious difference regarding the weight loss of chitosan-based specimens and their control counterparts. After 60 days, there is a significant difference between the weight losses of specimens that were in the lysozyme solution than their control specimens counterparts, pointing out the enzyme action in the degradation process, even for such high DD.

Besides the expected weight loss, the porosity of specimens is expected to increase with increasing of immersion time in the enzymatic solutions (Ding, 2007). *In vivo*, increasing chitosan-based implants porosity can improve cell proliferation, since the bone tissue cells could migrate into these structures, allowing implant osteointegration and accelerating its complete transformation into real bone tissue. The pore structure of the post-implantation biomaterial can also promote increase in vascularization, nutrient exchange between the surrounding tissues, and accelerate material degradation (Ding, 2007; Chen et al., 2010). Therefore, the chitosan-based porous structure that is expected to result from this degradation process can help the proliferation of cells. However, the initial mechanical performance of a chitosan-based implant also has to be taken into account, since an increase in the number of pores lead to a decrease in the mechanical properties (Ding, 2007).

To further investigate the effect of degradation on the above mentioned chitosan-based specimens, their modulus of elasticity (Fig. 5) and compressive strength (Fig. 6) were assayed. It is noteworthy that after 30 days none of the M specimens could be tested due to its severe physical degradation. These specimens, after drying, were so brittle that broke before testing. However, the control assays, where degradation is slower due to absence of lysozyme, can provide comparative information on the introduction of glycerol when preparing specimens with medium molecular weight chitosan. After 60 days, the M specimens in the control assays show a significant decrease in modulus of elasticity and compressive strength, whereas M+Gl specimens just suffered a slight decrease in the modulus of elasticity after the same period. Moreover, when immersed in PBS solution containing lysozyme the 60-day modulus of elasticity of the M+Gl specimens slightly declined from an average value of 467 MPa to 413 MPa.

As far as H-based specimens are concerned, the variations in the modulus of elasticity with immersion time revealed

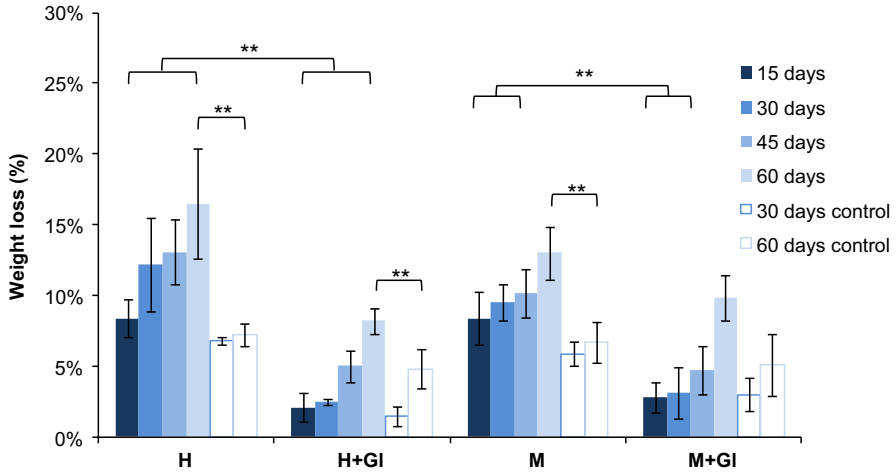

Fig. 4 – Weight loss (%) of chitosan-based specimens immersed in PBS supplemented with lysozyme (15, 30, 45 and 60 days) and immersed in a PBS control solution (30 and 60 days control) over 60 days.

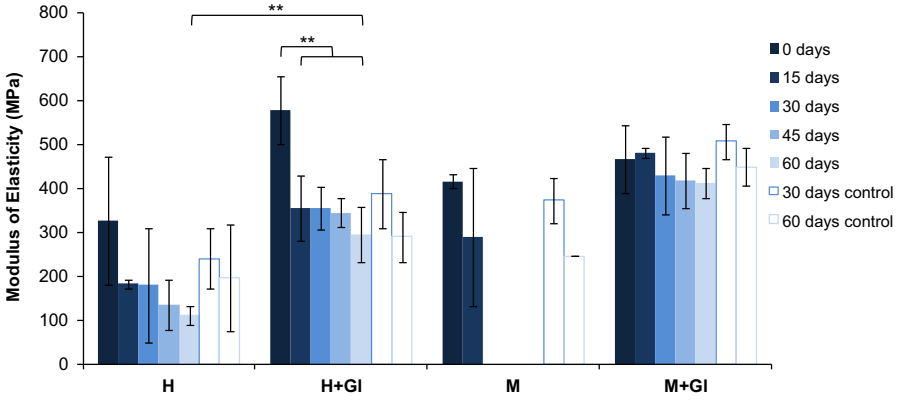

Fig. 5 – Modulus of elasticity (MPa) of chitosan-based specimens immersed in PBS supplemented with lysozyme (15, 30, 45 and 60 days) and immersed in a PBS control solution (30 and 60 days control) over 60 days.

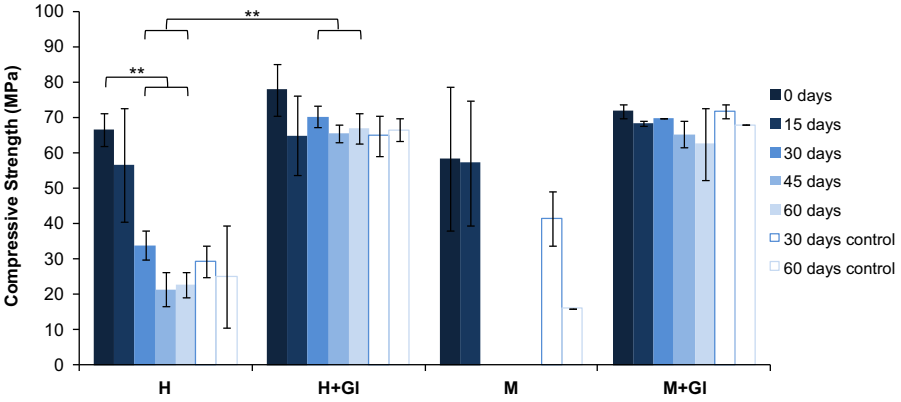

Fig. 6 – Compressive strength (MPa) of chitosan-based specimens immersed in PBS supplemented with lysozyme (15, 30, 45 and 60 days) and immersed in a PBS control solution (30 and 60 days control) over 60 days.

that, after immersion for 15 days, both H and H+Gl specimens largely declined the modulus of elasticity. For H specimens, the modulus of elasticity was significantly reduced from the initial average value of 328 MPa, down to 112 MPa, after 60 days immersion in the solution containing lysozyme. A similar trend can be observed for H+Gl specimens, although much higher absolute values of modulus of elasticity were obtained.

For the compressive strength, both H+Gl and M+Gl just faced a slight decrease throughout the experiments, confirming

the protective effect of glycerol. The highest changes were observed in the H specimens, for which compressive strength reduced to one-third of its initial value after 60 days. SEM images of H and H+Gl specimens after 60 days immersed in a PBS solution containing lysozyme and after being mechanically tested help explaining these results (Fig. 7). While H specimens become more and more brittle over time and therefore crack and fail at lower compressive stresses, H+Gl specimens compressive strength did not significantly changed since most of these specimens could handle the maximum compressive load – 10 kN – without breaking. As previously mentioned, most of M specimens could not be tested; however, when looking for the results of the control specimens after 60 days, it is expected that these specimens would have a similar behavior as H specimens. Therefore, the plasticized effect of glycerol seems to help maintaining the initial mechanical properties of specimens, over time, when these are immersed in a degradation solution.

In general, unplasticized chitosan specimens clearly presented a more brittle behavior than the plasticized ones. Moreover, the penetration of water/ions resulting from the solution could reduce the adhesion between interfaces, explaining the compressive strength decrease of pure chitosan specimens (Ding, 2007). The addition of glycerol influenced the mechanical properties of the specimens, particularly their strength. Both modulus of elasticity and compressive strength of M+Gl specimens underwent slight changes during the 60 days period. Thus, these specimens' composition might be an optimal material in terms of initial strength and degradation behavior for applications that need to keep the mechanical properties of the absorbable implant, at least, during the first two months. It is known that, for a long-term stability *in vivo*, a chitosan-based specimen would have to be composed by a chitosan with a high DD. Moreover, a high DD is also crucial to achieve high mechanical strength (Chen and Hwa, 1996; Freier et al., 2005). Besides that, there are several strategies to maintain the mechanical strength and preventing the premature collapse of specimens, such as the incorporation of polymer coils into the specimens (Freier et al., 2005), hydroxyapatite (Pu et al., 2012; Pradal et al., 2011), gelatin (Xu et al., 2013), the use of various cross-linking reagents (e.g. glutaraldehyde, ethylene glycol diglycidyl ether; diisocyanate; genipin) (Mi et al., 2001; Moura et al., 2007), among others. Fig. 8 represents an overview of the main results, showing that the incorporation of glycerol – 7.5% (v/v) – can improve the mechanical properties of chitosan-based specimens and slow down their degradation.

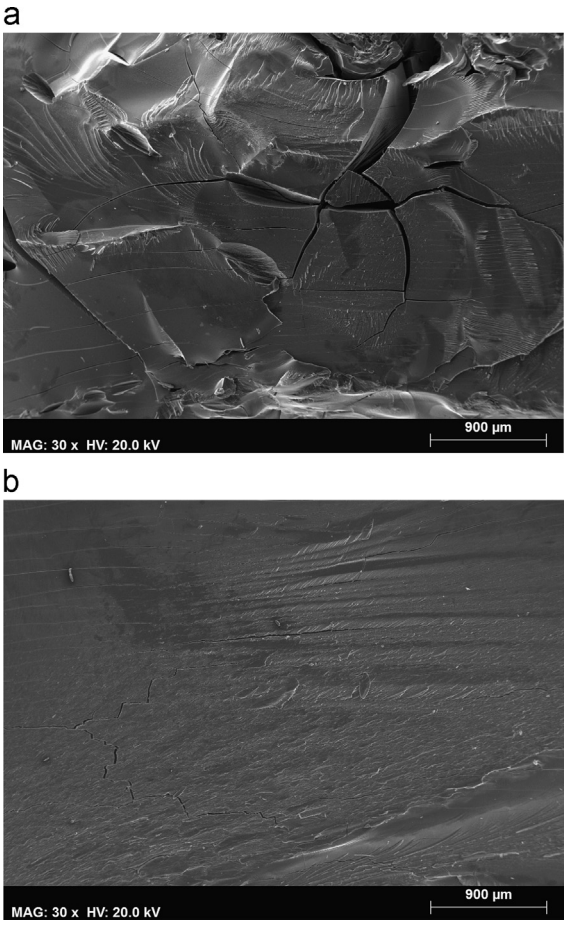

Fig. 7 – SEM images of (a) H and (b) H+Gl mechanically tested specimens, after 60 days immersed in a PBS solution containing lysozyme.

3.3. *In vitro cytotoxicity and cell proliferation on chitosan-based specimens*

In order to verify the cytotoxicity of the chitosan-based specimens, extract and direct cytotoxic assays were performed according to ISO 10993-5 guidelines for medical devices (Silva et al., 2005; Chen et al., 2010), using the fibroblast L929 cell line. Chitosan-based specimens were first tested in order to confirm that their production process and the variation in composition (chitosans with different molecular weight and glycerol) do not generate toxic compounds from these specimens. The results in Fig. 9 show that for all the specimens tested, cells' metabolic activity when exposed to lixiviates is maintained at high values comparable with the negative control (culture medium) and significant higher than the ones observed for the positive control (presence of cytotoxic material). These results indicated that the potential

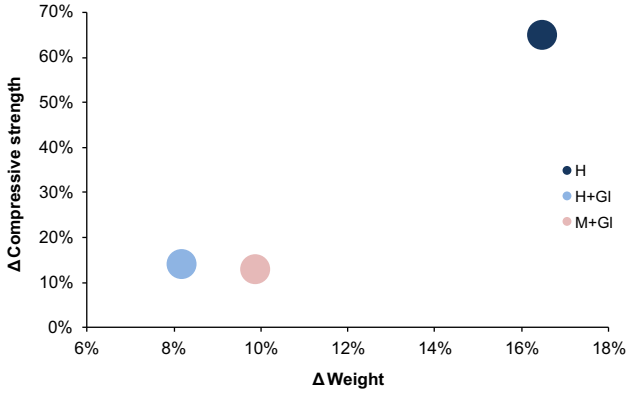

Fig. 8 – Variation of weight (Δ Weight) and variation of compressive strength (Δ Compressive strength) of tested chitosan-based structures after being immersed in PBS supplemented with lysozyme for 60 days (M specimens broke before being mechanically tested and are not represented).

lixiviates from the chitosan-based specimens had no obvious cytotoxic effect, regardless their composition, and therefore further tests where the specimens were put in direct contact with the cells were performed.

The result of the direct contact assay is shown in Fig. 10, where no inhibition halo resulting from cell death around the chitosan-based specimens was observed. These specimens remained fully transparent by light microscopy, allowing for a direct observation of the cell morphology and growth throughout the material. Since no morphologic alteration or effects on cell proliferation were observed, it was considered that the tested specimens were neither cytotoxic towards the cells, nor released cytotoxic substances in the culture medium.

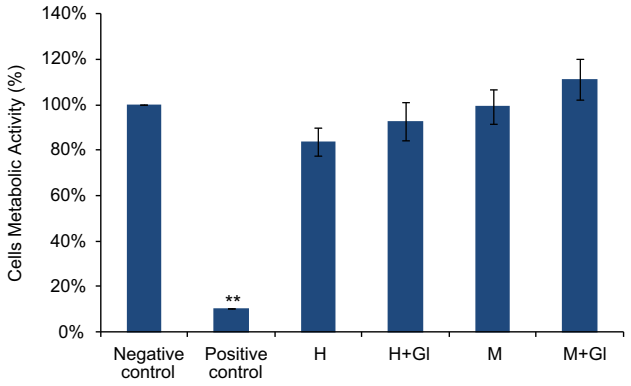

Fig. 9 – Cytotoxicity results for MTT assay of chitosan-based specimens.

Previous studies have demonstrated that DD has no significant influence on the *in vitro* cytocompatibility of chitosan films towards fibroblasts, confirming the biocompatibility of chitosan-based materials regardless the DD. It is also suggested that DD would also have no effect *in vivo*, or towards other cell types (Chatelet et al., 2001; Dash et al., 2011). However, at high DD, the toxicity is related to the molecular weight and polymer concentration (Dash et al., 2011). In this study, none of the chitosan-based specimens induced a cytotoxic effect. Besides the nontoxic nature and biocompatibility of chitosan, its processability into geometrically different structures is an important aspect for biomedical applications. Structures made from pure chitosan are rigid and brittle, and it is therefore important to use plasticizers in order to obtain more favorable mechanical properties. Because of the potential medical applications, the plasticizer materials must be biocompatible as well (Domján et al., 2009). The results presented in this study showed that glycerol is an effective and biocompatible plasticizer for

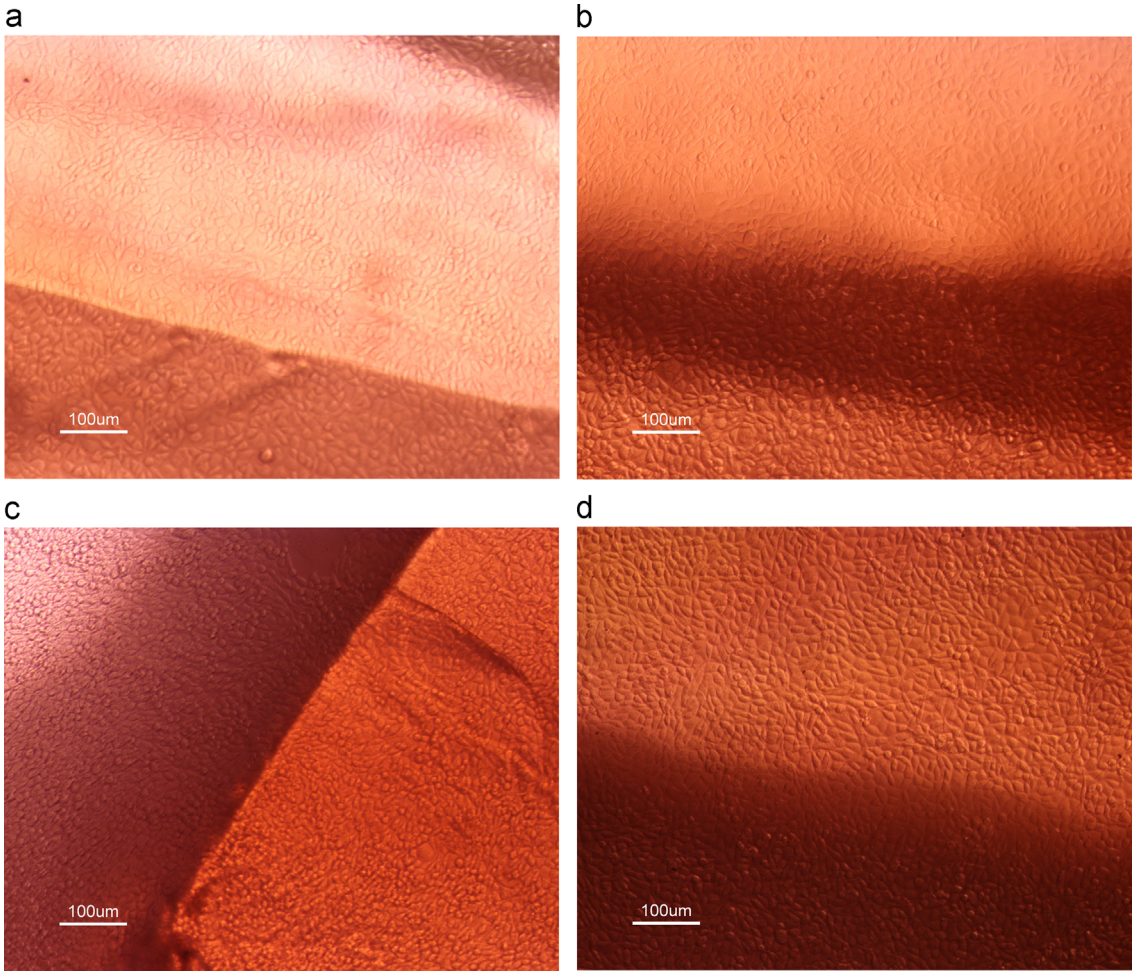

Fig. 10 – Cytotoxicity assays for direct contact assay of chitosan-based specimens: (a) cells cultured on H; (b) cells cultured on H+Gl; (c) cells cultured on M; (d) cells cultured on M+Gl.

rigid and brittle chitosan specimens, without compromising cytocompatibility.

Preliminary experiments were also conducted to study the proliferation of bone marrow (BM) mesenchymal stem/stromal cells (MSC) on chitosan-based specimens. M and M+GI specimens were selected for this assay, allowing testing the effect of glycerol on one of the chitosan types studied. MSC were also plated and cultured on common Polystyrene (PS) tissue culture (TC) plates for comparison. From day 1 to day 10, the cellular expansion was 3.7 ± 0.4, 5.5 ± 2.0 and 6.7 ± 3.1 fold for cultures in PS TC, M and M+GI specimens, respectively (where fold increase was defined as the ratio between cells at day 10 and 1). These values correspond to $(160 \pm 5) \times 10^3$, $(75 \pm 20) \times 10^3$ and $(84 \pm 17) \times 10^3$ cells estimated for cultures on PS TC, M and M+GI specimens, respectively. At day 1, the amount of cells was about 3.2 times higher on PS TC ($(45 \pm 4) \times 10^3$ cells) than on the tested chitosan specimens – (14 ± 2) and $(13 \pm 3) \times 10^3$ cells for M and M+GI specimens, respectively – which can result from a different initial adhesion to PS TC. Note that PS TC used is a commercial product in which polarity has been adjusted using plasma treatment for optimal cell adhesion. The initial cell adhesion may have an impact on observed cell proliferation, since the lower cell density in chitosan samples may had contribute to higher fold increase values in MSC cultures in chitosan when compared to PS TC. Briefly, although the studied chitosan-based specimens support MSC adhesion and proliferation, further assays are required to test whether the use of different chitosan molecular weight, or the introduction of different amounts of glycerol would promote different cell responses, namely concerning maintenance of multipotency and allow eventual osteo-differentiation.

4. Conclusion

Four different kinds of chitosan-based specimens – H; H+Gl; M; M+Gl – were successfully prepared and characterized in this study. Both physical and biological results obtained suggest that chitosan-based specimens, particularly the M+Gl specimens (7.5% (v/v) of glycerol), might be an optimal material in terms of initial strength and degradation behavior for applications that need to keep the mechanical properties of the absorbable implant, at least, during the first two months. Furthermore, besides the non-cytotoxic effect of these specimens, preliminary experiments showed that MSC effectively adhere and proliferate on the chitosan structures at similar level in plasticized and non-plasticized structures. From the results obtained for these chitosan-based specimens, several potential biomedical applications could be pointed out. Taking into account the mechanical properties of the tested specimens and the mechanical properties of bone, one can assert that they are in between cancellous bone—compressive strength: 2–12 MPa and Young's modulus: 50–500 MPa–and cortical bone—compressive strength: 100–230 MPa and Young's modulus: 7–30 GPa (Kokubo et al., 2003). Considering such values, knowing that the vertebral cortical bone *in vivo* has a thickness often less than 0.4 mm and the apparent Young's modulus (computed by a finite element method (FEM) inverse analysis) is equal to, on average, 374 MPa (SD=208) (El Masri et al., 2012), chitosan-based implants for spine, such as absorbable spinal cages, could be an appealing application. Spinal fusion is considered to be one of the most challenging applications for bone graft substitutes, since even the transplant of autologous bone, the current golden standard treatment, has a relatively high rate of failure (Kruyt et al., 2004). An ideal scenario for interbody fusion is a cage device that (i) has a modulus of elasticity as close as to that of vertebral bone, (ii) will be absorbed after interbody fusion and (iii) will be replaced by new cancellous bone, not leaving foreign body material in the spinal segment (Van Dijk et al., 2003). Thus, the plasticized chitosan-based specimens seem to be an appealing alternative to the existing materials. Moreover, MSC, which are the osteoprogenitor cells responsible for bone fusion and have been identified in vertebra (Nguyen and Fleischer, 2012), have shown to proliferate well on 3D plasticized chitosan-based structures.

In conclusion, although interesting results were obtained, suggesting that chitosan-based spinal cages for interbody fusion could be an appealing application, further *in vitro* and *in vivo* long-term experiments are needed not only to optimize the biological properties, but also the degradation and biomechanical properties of these structures. It is required to guarantee that these degradable devices possess adequate mechanical properties that are gradually lost during the degradation process to progressively transfer mechanical loads to the newly forming bone. They should also provide appropriate surface chemistry to facilitate cell attachment, proliferation, and differentiation throughout the bone healing (or fusion) process.

Acknowledgments

Authors would like to thank Altakitin S.A. for the support and for the material that has been provided. Special thanks to Samuel Jorge from the Bioengineering Research Group (BERG) of IST for being available to help and give support during the lab experiments. N G Oliveira and F C Ferreira gratefully acknowledges Fundação para a Ciência e Tecnologia (FCT) for the grant SFRH/BD/33732/2009 and research contract "Investigador FCT" Program (IF/00442/2012), respectively.

This project has received funding from the European Union's Seventh Programme for research, technological development and demonstration under grant agreement no. 278612.

REFERENCES

Abbah, S.a., Lam, C.X.L., Hutmacher, D.W., Goh, J.C.H., Wong, H.-K., 2009. Biological performance of a polycaprolactone-based scaffold used as fusion cage device in a large animal model of spinal reconstructive surgery. Biomaterials 30, 5086–5093.

Albanna, M.Z., Bou-Akl, T.H., Blowytsky, O., Walters, H.L., Matthew, H.W.T., 2013. Chitosan fibers with improved biological and mechanical properties for tissue engineering applications. J. Mech. Behav. Biomed. Mater. 20, 217–226.

Ambrose, C.G., Clanton, T.O., 2004. Bioabsorbable implants: review of clinical experience in orthopedic surgery. Ann. Biomed. Eng. 32, 171–177.

Bajdik, J., Marciello, M., Caramella, C., Domján, A., Süvegh, K., Marek, T., Pintye-Hódi, K., 2009. Evaluation of surface and microstructure of differently plasticized chitosan films. J. Pharm. Biomed. Anal. 49, 655–659.

Böstman, O., Pihlajamäki, H., 2000. Clinical biocompatibility of biodegradable orthopaedic implants for internal fixation: a review. Biomaterials 21, 2615–2621.

Canadas, R.F., Cavalheiro, J.M., Guerreiro, J.D., Almeida, M.C., Pollet, E., Silva, C.L., Fonseca, M.M., Ferreira, F.C., 2014. Polyhydroxyalkanoates: waste glycerol upgrade into electrospun fibrous scaffolds for stem cells culture. Int. J. Biol. Macromol. (In Press) (Available online: 14 May 2014).

Caplan, A.I., 1991. Mesenchymal stem cells. J. Orthop. Res. 9, 641–650.

Chatelet, C., Damour, O., Domard, A., 2001. Influence of the degree of acetylation on some biological properties of chitosan films. Biomaterials 22, 261–268.

Chen, H., Zhao, Z., Zhao, Y., Yang, Y., 2010. Fabrication and evaluation of chitosan-gelatin based buckling implant for retinal detachment surgery. J. Mater. Sci. Mater. Med. 21, 2887–2895.

Chen, R.H., Hwa, H.-D., 1996. Effect of molecular weight of chitosan with the same degree of deacetylation on the thermal, mechanical, and permeability properties of the prepared membrane. Carbohydr. Polym. 29, 353–358.

Chesnutt, B.M., Viano, A.M., Yuan, Y., Yang, Y., Guda, T., Appleford, M.R., Ong, J.L., Haggard, W.O., Bumgardner, J.D., 2009. Design and characterization of a novel chitosan/nanocrystalline calcium phosphate composite scaffold for bone regeneration. J. Biomed. Mater. Res. A 88, 491–502.

Cheung, H.-Y., Lau, K.-T., Lu, T.-P., Hui, D., 2007. A critical review on polymer-based bio-engineered materials for scaffold development. Composites Part B 38, 291–300.

Correia, C.R., Moreira-Teixeira, L.S., Moroni, L., Reis, R.L., van Blitterswijk, C.a., Karperien, M., Mano, J.F., 2011. Chitosan scaffolds containing hyaluronic acid for cartilage tissue engineering. Tissue Eng. Part C 17, 717–730.

Dash, M., Chiellini, F., Ottenbrite, R.M., Chiellini, E., 2011. Chitosan—a versatile semi-synthetic polymer in biomedical applications. Prog. Polym. Sci. 36, 981–1014.

De Souza Costa-Júnior, E., Pereira, M.M., Mansur, H.S., 2009. Properties and biocompatibility of chitosan films modified by blending with PVA and chemically crosslinked. J. Mater. Sci. Mater. Med. 20, 553–561.

Di Martino, A., Sittinger, M., Risbud, M.V., 2005. Chitosan: a versatile biopolymer for orthopaedic tissue-engineering. Biomaterials 26, 5983–5990.

Ding, S.-J., 2007. Biodegradation behavior of chitosan/calcium phosphate composites. J. Non-Cryst. Solids 353, 2367–2373.

Domján, A., Bajdik, J., Pintye-Hódi, K., 2009. Understanding of the Plasticizing Effects of Glycerol and PEG 400 on Chitosan Films Using Solid-State NMR Spectroscopy. Macromolecules 42, 4667–4673.

Eglin, D., Alini, M., 2008. Degradable polymeric materials for osteosynthesis: tutorial. Eur. Cell Mater. 16, 80–91.

El Masri, F., Sapin de Brosses, E., Rhissassi, K., Skalli, W., Mitton, D., 2012. Apparent Young's modulus of vertebral cortico-cancellous bone specimens. Comput. Meth. Biomech. Biomed. Eng. 15, 23–28.

Epure, V., Griffon, M., Pollet, E., Avérous, L., 2011. Structure and properties of glycerol-plasticized chitosan obtained by mechanical kneading. Carbohydr. Polym. 83, 947–952.

Freier, T., Montenegro, R., Shan Koh, H., Shoichet, M.S., 2005. Chitin-based tubes for tissue engineering in the nervous system. Biomaterials 26, 4624–4632.

Freier, T., Koh, H.S., Kazazian, K., Shoichet, M.S., 2005. Controlling cell adhesion and degradation of chitosan films by N-acetylation. Biomaterials 26, 5872–5878.

Greenwald, R.A., Josephson, A.S., Diamond, H.S., Tsang, A., 1972. Human cartilage lysozyme. J. Clin. Invest. 51, 2264–2270.

Guitian Oliveira, N., Rodrigues, A., Reis, L., Pinto, L.F.V., 2013. Trends in bioabsorbable osteosynthesis devices: introduction to a novel production process of chitosan-based implants. J. Chitin Chitosan Sci. 1, 210–220.

Hasirci, V., Lewandrowski, K., Gresser, J.D., Wise, D.L., Trantolo, D.J., 2001. Versatility of biodegradable biopolymers: degradability and an in vivo application. J. Biotechnol. 86, 135–150.

Hirai, A., Odani, H., Nakajima, A., 1991. Determination of degree of deacetylation of chitosan by 1H NMR spectroscopy. Polym. Bull. 26, 87–94.

Hsieh, W.-C., Chang, C.-P., Lin, S.-M., 2007. Morphology and characterization of 3D micro-porous structured chitosan scaffolds for tissue engineering. Colloids Surf., B 57, 250–255.

Hu, Q., Li, B., Wang, M., Shen, J., 2004. Preparation and characterization of biodegradable chitosan/hydroxyapatite nanocomposite rods via in situ hybridization: a potential material as internal fixation of bone fracture. Biomaterials 25, 779–785.

Itoh, S., Yamaguchi, I., Shinomiya, K., Tanaka, J., 2003. Development of the chitosan tube prepared from crab tendon for nerve regeneration. Sci. Technol. Adv. Mater. 4, 261–268.

Khor, E., Lim, L.Y., 2003. Implantable applications of chitin and chitosan. Biomaterials 24, 2339–2349.

Kim, I.-Y., Seo, S.-J., Moon, H.-S., Yoo, M.-K., Park, I.-Y., Kim, B.-C., Cho, C.-S., 2008. Chitosan and its derivatives for tissue engineering applications. Biotechnol. Adv. 26, 1–21.

Knaul, J.Z., Kasaai, M.R., Bui, V.T., Creber, K.A.M., 1998. Characterization of deacetylated chitosan and chitosan molecular weight review. Can. J. Chem. 76, 1699–1706.

Kokubo, T., Kim, H.-M., Kawashita, M., 2003. Novel bioactive materials with different mechanical properties. Biomaterials 24, 2161–2175.

Kolhe, P., Kannan, R.M., 2003. Improvement in ductility of chitosan through blending and copolymerization with PEG: FTIR investigation of molecular interactions. Biomacromolecules 4, 173–180.

Kruyt, M.C., van Gaalen, S.M., Oner, F.C., Verbout, A.J., de Bruijn, J.D., Dhert, W.J.a., 2004. Bone tissue engineering and spinal fusion: the potential of hybrid constructs by combining osteoprogenitor cells and scaffolds. Biomaterials 25, 1463–1473.

Lim, S.M., Song, D.K., Oh, S.H., Lee-Yoon, D., Bae, E.H., Lee, J.H., 2008. In vitro and in vivo degradation behavior of acetylated chitosan porous beads. J. Biomater. Sci., Polym. Ed. 19, 453–466.

Lippman, C.R., Hajjar, M., Abshire, B., Martin, G., Engelman, R.W., Cahill, D.W., 2004. Cervical spine fusion with bioabsorbable cages. Neurosurg. Focus 16, E4.

Martins, A.M., Alves, C.M., Kurtis Kasper, F., Mikos, A.G., Reis, R.L., 2010. Responsive and in situ-forming chitosan scaffolds for bone tissue engineering applications: an overview of the last decade. J. Mater. Chem. 20, 1638–1645.

Mi, F.L., Tan, Y.C., Liang, H.C., Huang, R.N., Sung, H.W., 2001. In vitro evaluation of a chitosan membrane cross-linked with genipin. J. Biomater. Sci., Polym. Ed. 12, 835–850.

Moura, M.J., Figueiredo, M.M., Gil, M.H., 2007. Rheological study of genipin cross-linked chitosan hydrogels. Biomacromolecules 8, 3823–3829.

Mukherjee, D., Pietrzak, W., 2011. Bioabsorbable fixation: scientific, technical, and clinical concepts. J. Craniofac. Surg. 22, 679–689.

Nair, L.S., Laurencin, C.T., 2007. Biodegradable polymers as biomaterials. Prog. Polym. Sci. 32, 762–798.

Nguyen, D.T., McCanless, J.D., Mecwan, M.M., Noblett, a.P., Haggard, W.O., Smith, R.a., Bumgardner, J.D., 2013. Balancing mechanical strength with bioactivity in chitosan-calcium phosphate 3D microsphere scaffolds for bone tissue engineering: air- vs. freeze-drying processes. J. Biomater. Sci., Polym. Ed. 24, 1071–1083.

Nguyen, T.T., Fleischer, G.D., 2012. Isolation of mesenchymal stem cells expressing BMPs from vertebra and Iliac crest during spinal fusion. Spine J. 12, 21S.
Nunthanid, J., Puttipipatkhachorn, S., Yamamoto, K., Peck, G.E., 2001. Physical properties and molecular behavior of chitosan films. Drug Dev. Ind. Pharm. 27, 143–157.
Oh, D.X., Hwang, D.S., 2013. A biomimetic chitosan composite with improved mechanical properties in wet conditions. Biotechnol. Prog. 29, 505–512.
O'Brien, J., Wilson, I., Orton, T., Pognan, F., 2000. Investigation of the Alamar Blue (resazurin) fluorescent dye for the assessment of mammalian cell cytotoxicity. Eur. J. Biochem. 267, 5421–5426.
Park, B.K., Kim, M.-M., 2010. Applications of chitin and its derivatives in biological medicine. Int. J. Mol. Sci. 11, 5152–5164.
Pradal, C., Kithva, P., Martin, D., Trau, M., Grøndahl, L., 2011. Improvement of the wet tensile properties of nanostructured hydroxyapatite and chitosan biocomposite films through hydrophobic modification. J. Mater. Chem. 21, 2330–2337.
Pu, X.-M., Sun, Z.-Z., Hou, Z.-Q., Yang, Y., Yao, Q.-Q., Zhang, Q.-Q., 2012. Fabrication of chitosan/hydroxylapatite composite rods with a layer-by-layer structure for fracture fixation. J. Biomed. Mater. Res. B Appl. Biomater. 100, 1179–1189.
Pu, X.-M., Yao, Q.-Q., Yang, Y., Sun, Z.-Z., Zhang, Q.-Q., 2012. In vitro degradation of three-dimensional chitosan/apatite composite rods prepared via in situ precipitation. Int. J. Biol. Macromol. 51, 868–873.
Qu, J., Hu, Q., Shen, K., Zhang, K., Li, Y., Li, H., Zhang, Q., Wang, J., Quan, W., 2011. The preparation and characterization of chitosan rods modified with Fe3+ by a chelation mechanism. Carbohydr. Res. 346, 822–827.
Quijada-Garrido, I., Laterza, B., Mazón-Arechederra, J.M., Barrales-Rienda, J.M., 2006. Characteristic features of chitosan/glycerol blends dynamics. Macromol. Chem. Phys. 207, 1742–1751.
Ralph, P., Moore, M.A., Nilsson, K., 1976. Lysozyme synthesis by established human and murine histiocytic lymphoma cell lines. J. Exp. Med. 143, 1528–1533.
Ren, D., Yi, H., Wang, W., Ma, X., 2005. The enzymatic degradation and swelling properties of chitosan matrices with different degrees of N-acetylation. Carbohydr. Res. 340, 2403–2410.
Reves, B.T., Jennings, J.a., Bumgardner, J.D., Haggard, W.O., 2012. Preparation and functional assessment of composite chitosan-nano-hydroxyapatite scaffolds for bone regeneration. J. Funct. Biomater. 3, 114–130.
Robbins, M.M., Vaccaro, A.R., Madigan, L., 2004. The use of bioabsorbable implants in spine surgery. Neurosurg. Focus 16, E1.
Sigma-Aldrich Lysozyme human.
Silva, S.S., Santos, M.I., Coutinho, O.P., Mano, J.F., Reis, R.L., 2005. Physical properties and biocompatibility of chitosan/soy blended membranes. J. Mater. Sci. - Mater. Med. 16, 575–579.
Vaccaro, A.R., Singh, K., Haid, R., Kitchel, S., Wuisman, P., Taylor, W., Branch, C., Garfin, S., 2003. The use of bioabsorbable implants in the spine. Spine J. 3, 227–237.
Van Dijk, M., Tunc, D.C., Smit, T.H., Higham, P., Burger, E.H., Wuisman, P I J M, 2002. In vitro and in vivo degradation of bioabsorbable PLLA spinal fusion cages. J. Biomed. Mater. Res. 63, 752–759.
Van Dijk, M., Smit, T.H., Arnoe, M.F., Burger, E.H., Wuisman, P.I., 2003. The use of poly-L-lactic acid in lumbar interbody cages: design and biomechanical evaluation in vitro. Eur. Spine J. 12, 34–40.
Wang, Z., Hu, Q., 2010. Preparation and properties of three-dimensional hydroxyapatite/chitosan nanocomposite rods. Biomed. Mater. 5, 045007.
Wang, Z., Hu, Q., Cai, L., 2010. Chitin fiber and chitosan 3D composite rods. Int. J. Polym. Sci. 2010, 1–7.
Wuisman, P.I.J.M., Smit, T.H., 2006. Bioresorbable polymers: heading for a new generation of spinal cages. Eur. Spine J. 15, 133–148.
Xu, T., Yang, Y., Yu, Y., Zhu, R., Chen, H.U.I., 2013. Efficacy, safety, and biodegradation of a degradable scleral buckle of chitosan-gelatin polymer in rabbits. Retina 33, 1062–1069.
Zhang, M., Li, X.H., Gong, Y.D., Zhao, N.M., Zhang, X.F., 2002. Properties and biocompatibility of chitosan films modified by blending with PEG. Biomaterials 23, 2641–2648.